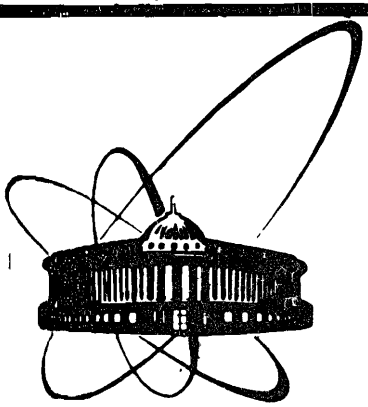

объединенный
институт
ядерных
исследований
дубна

E4-87-517

V.V.Pashkevich

PRESCISSION SHAPES OF SYMMETRICALLY FISSIONING VERY HEAVY NUCLEI

Submitted to "Nuclear Physics"

1987

I. Introduction

In ref. [1] it has been shown experimentally that some nuclei with $Z \geq 100$ and $N \geq 156$ fission in two different ways. Both fission modes were shown to have symmetric mass distributions of the fission fragments, one distribution being narrow and the other broad. The fission mode having a narrow mass distribution is characterized by an abnormally large value of the total kinetic energy (TKE), while the broad distribution corresponds to the usual TKE values which may be expected from the systematics [2]. Two fission modes in one nucleus have also been observed in light pre-actinides [3,4].

The theoretical consideration of the potential energy surface led to the conclusion that there are two saddle points on this surface for nuclei in the lead region, which correspond to nearly symmetric and highly asymmetric fission [5]. Analogous calculations were carried out in the present paper for the heavier nuclei in order to show that both of the experimentally observed modes may be described in a unified manner by using the Strutinsky shell correction method.

The main results were obtained for ^{264}Fm which has so far not been observed experimentally and the fission of which can reasonably be assumed to be subject to the strongest influence of the fragment shells. Preliminary results limited to the reflection symmetric shapes were published in ref. [6]. Most of the data obtained here were reported at the International School-Seminar of Heavy Ion Physics at Dubna in September 1986 [7].

Similar results restricted to reflection-symmetric shapes were reported at the same conference (see ref. [8]). Several modes of fission in ^{258}Fm have also been considered recently in a simple parameterization of the nuclear shape [9].

2. Method of calculating the deformation energy

The nuclear deformation energy, E, was calculated by the Strutinsky method [10,11], i.e.

$$E = E_{LD} + \delta E, \qquad (1)$$

where E_{LD} is the energy in the liquid drop model with parameters from ref. [12,13] (the surface, Coulomb and symmetry constants

are α_2=17.9439, C_3=0.7053 and $\varkappa$=1.78, respectively) and δE is the shell correction calculated with a Woods-Saxon type potential /14-16/, the parameters being taken from ref. /17/.

The accuracy of the single-particle spectrum calculation and the plateau condition formulated by Strutinsky for δE were checked near the scission point and the results are discussed in Appendices A and B.

3. Shape parameterization

For the description of the expected variety of shapes one needs a rather unrestrictive parameterization. For this purpose the coordinate system based on Cassinian ovals /5/ is used, in which a point on the plane is defined by the coordinates (R, x). If the distance between the foci of Cassinian ovals equals zero, then (R, x) is transformed into the spherical radius and the cosine of the polar angle. The expression for (R, x) in terms of the cylindrical coordinates was given in ref. /5/ (see also /18/). The intersection of the surface of an axially symmetric nucleus with the plane passing through the symmetry axis is described by the equation

$$R = R(x), \quad -1 \le x \le 1. \tag{2}$$

In the particular case of the nuclear surface being approximated by a Cassinian oval, eq. (2) takes on the simple form

$$R = \text{const}. \tag{3}$$

A more general class of nuclear surfaces may be described by the series

$$R = \frac{R_0}{c}\left(1 + \sum_m \alpha_m P_m(x)\right), \tag{4}$$

where R_0 is the radius of the sphere of the same volume, c is to be eliminated by volume conservation, $P_m(x)$ are the Legendre polynomials and α_m are the parameters which specify the shape of the nucleus. The elongation of the nucleus is characterized by the squared half-distance ε between the foci of the Cassinian ovals (in units of R_0^2).

Near the scission point of a reflection-symmetric figure it is convenient to use as an independent variable, instead of ε, the parameter α defined as follows

$$\alpha = \frac{z_L^2 + z_R^2 - 2\varrho}{z_L^2 + z_R^2 + 2\varrho}, \tag{5}$$

where z_L (z_R) is the minimum (maximum) value of the cylindrical coordinate z and $\varrho = r_{neck}^2$, r_{neck} being the radius of the cross section of the nuclear surface by the plane $z = 0$, in the case of a connected body. For a two-fragment shape ϱ is defined as minus the square of half the distance between the fragments. The relation between α and ε can be derived from (5) using the connection of the (R, x)-coordinates with the cylindrical coordinates /5/

$$\varepsilon = \frac{\alpha - 1}{4}\left[\left(1 + \sum_m \alpha_m\right)^2 + \left(1 + \sum_m (-1)^m \alpha_m\right)^2\right] + \tag{6}$$

$$+ \frac{\alpha + 1}{2}\left[1 + \sum_{m=1} (-1)^m \alpha_{2m} (2m-1)!!/(2^m m!)\right]^2,$$

which will be used here also for reflection-asymmetric shapes.

The advantage of the parameter α results from the fact that for a shape with vanishing neck ($r_{neck} = 0$) α equals 1 for any value of α_m. For the spherical shape one obtains $\alpha = 0$ because $r_{neck} = z_R = |z_L|$.

The minimization of the energy E with respect to a large number of parameters α_m takes many hours of computer time and, therefore, the consideration has been limited to the most important region lying in the vicinity of the scission point, which, after the introduction of the parameter α, can be characterized conveniently by the α values close to 1.

4. Existence and relative position of the fission valleys

Strictly speaking, the concept of a valley in a potential energy surface is dependent on the coordinate system, in contrast to an extremum. So we should specify what we mean by the "fission valley". We define it as a local minimum in the multidimensional space of the shape parameters α_m at a fixed value of the parameter α. Moreover, the valley defined in this way is physically meaningful only if it is surrounded by a sufficiently high barrier that separates it from other regions.

A search for local minima with the constraint $\alpha = 0.98$ reveals in ^{264}Fm the existence of at least three valleys leading to scission . The search was carried out as follows.

First, the deformation energy E and the liquid-drop energy E_{LD} were calculated as functions of the hexadecapole deformation α_4 and the result is shown in fig.1. It is seen that E has two minima, one being deep and the other being shallow. The depth and position of

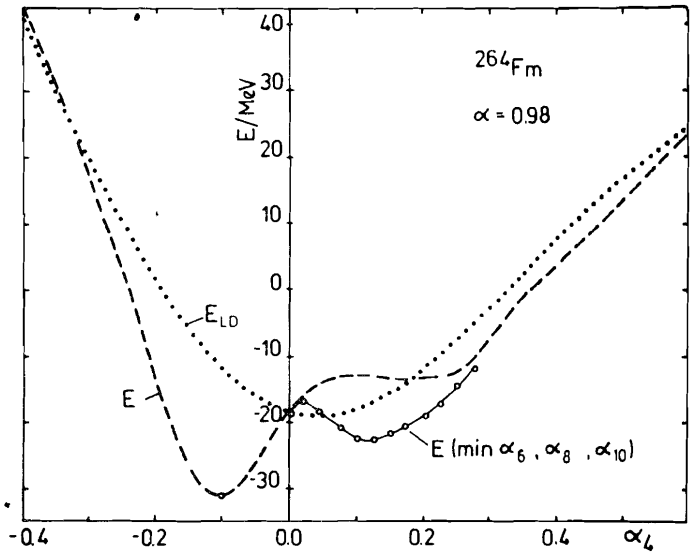

Fig.1

The deformation energy (in MeV) in the liquid-drop model, E_{LD} (dots), and with shell correction, E (dashed and solid curves), as a function of hexadecapole deformation α_4 at fixed elongation $\alpha = 0.98$. The solid curve with open circles corresponds to minimization with respect to α_6, α_8 and α_{10}.

the deep minimum remains almost unchanged after taking into account the higher deformations α_m, while minimization with respect to α_6, α_8 and α_{10} leads to a shift in the position and to a strong deepening of the shallow minimum (open points connected by a solid curve in fig.1). After taking into account higher deformations up to α_{20} this minimum deepens further (cf. fig.3).

Second, the calculations were repeated with reflection asymmetric shapes . The deep minimum remains almost unaffected. The corresponding shape marked as I is shown in fig.2. It is seen

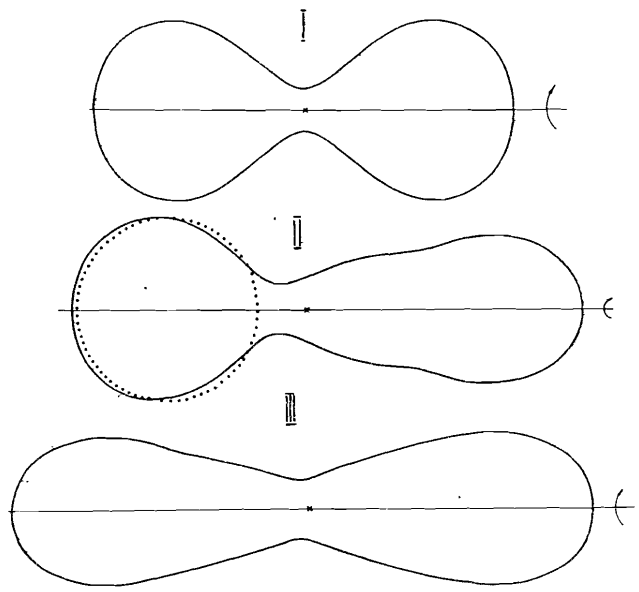

Fig.2

The nuclear shape of ^{264}Fm near the scission point, $\alpha = 0.98$, in the three valleys. Minimization of E with respect to $\alpha_1 - \alpha_{10}$ (I and II) and $\alpha_1 - \alpha_{20}$ (III) was carried out (with $\alpha_2 = 0$). A half-volume sphere is shown by dots for comparison.

that each of the two fragments has a shape close to sphericity .

In addition, a deep minimum has been found corresponding to a very asymmetric shape with one nearly spherical and one strongly deformed fragment, the corresponding shape being marked by II in fig.2.

The shallow minimum acquires a slightly asymmetric shape which is labeled as III in fig.2 and consists of two elongated fragments, one of them being very close in shape to the elongated fragment of shape II. In all the multiparameter calculations the α_2 parameter remains fixed and equal to zero, because its small variations are strongly correlated with those of α .

The relative height in energy of the three valleys and the upper estimates of the barriers between them are demonstrated in fig.3. There are shown the results of the calculation of the energy E along the intervals of straight lines that connect the three points in the multidimensional space of the shape parameters $\{\alpha_m\}$ corresponding to the three valleys. In view of the absence of

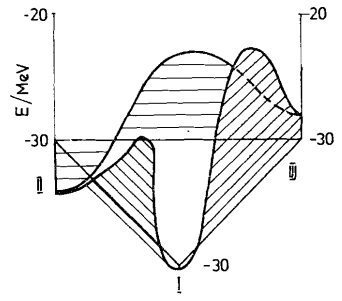

Fig.3.

A cut of the deformation energy surface E for the nucleus ^{264}Fm along the sides of a triangle in the 19-dimensional space of the shape parameters $\{\alpha_m, m=1,\dots,20\}$ ($\alpha_2=0$), the triangle vertices lying in valleys I, II and III are defined in the text; see also fig.2 ($\alpha = 0.98$). For simplicity, in valleys I and II the higher deformations are equal to zero, $\alpha_m=0$, m = 11, ..., 20.

a metric in the static approach in the space $\{\alpha_m\}$ the distances between the points lying in the vertices of the triangle in fig.3 are given in arbitrary units. The energy E calculated along the sides of the triangle in each of the three cases has a maximum that gives an upper limit for the estimate of the saddle point between the corresponding valleys. Assuming that the true saddle-point energies, although smaller, are of the same order in magnitude as the maxima in fig.3 we may conclude that all three valleys are well separated in energy from each other.

It is also seen from fig. 3 that valley I of compact configurations of almost spherical fragments occupies an intermediate position in energy and that the experimentally yet unobserved valley III is located higher in energy (-28 MeV) that both valleys II (-34 MeV) and I (-30 MeV).

The fragment of the plot in fig.3 is shown in more detail in fig.4 where the energies E for some other nuclei along the same

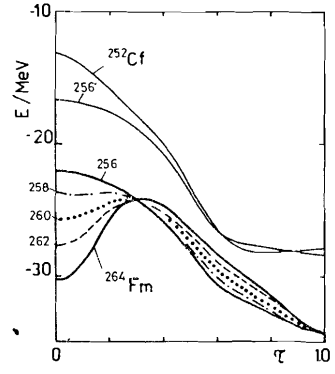

Fig.4.

The deformation energies E of the nuclei indicated in the figure along the interval of the straight line connecting two points in the 9-dimensional space $\{\alpha_m, m=1,\dots,10\}$ ($\alpha_2=0$) of the shape parameters, one of which lies in valley I (at $\tau = 0$ on the plot) and the other in valley II (at $\tau=1.0$), where τ is a parameter that specifies the position of a point in the interval, $\tau \in [0,1]$. The parameter $\alpha=0.98$ (see also the caption to fig.3).

space interval connecting minima I and II in the multidimensional space are also given. For the other nuclei the end points are not the loci of extrema of the potential energy surface but they are close to them if the corresponding extrema, as is the case indeed, are close to each other in the multidimensional space considered. The energies E calculated in this way are somewhat better approximations for the true extreme energies in fermium isotopes and not so good for californium, as it can be inferred from fig.4. However, this picture gives a rough idea of the relative position of the valleys in the other nuclei.

It is seen that in the californium isotopes there exists no valley, corresponding to a compact configuration of two almost spherical fragments; a minimum at the left-hand side is transformed into the maximum that lies 10-15 MeV higher in energy than the right-hand minimum does. Thus, in spite of all the approximations used one can conclude that the theory is capable of explaining the experimentally established absence of symmetric fission corresponding to fragments of unusually high TKE in ^{252,256}Cf /19/. An analogous conclusion can be drawn for ^{256}Fm as well. On the other hand, the existence of two valleys separated by a barrier is seen in $^{260-264}$Fm. The isotope ^{258}Fm occupies an intermediate position and in view of all uncertainties it is impossible to draw a definite conclusion about it from fig.4. From the experiment this nucleus is known to fission symmetrically /1/. So it appears possible to explain the existence of the two modes of fission /1/ in the heavy fermium isotopes by using a multiparametric description of the nuclear shape.

Let us note for comparison that in the two-centre oscillator model with limited parameterization of the nuclear shape on the potential energy surface only one valley was shown and emphasized corresponding either to symmetric or asymmetric fission /20/. In ref./21/ no valley has been found where one or both fragments are highly deformed. However the possibilities of the model are not exhausted (private communication by M.G.Mustafa).

It is interesting to note that before an isolated valley in lighter fermium isotopes appears at the corresponding position there exists a depression on the potential energy surface that may manifest itself in the experiment as a broadening of the distributions, i.e. the occurrence of symmetric fission with large TKE as low-probability events on the tail of the distribution. These events have been observed in ^{257}Fm experimentally /22/.

The probability of fission through one or another valley is a more delicate problem. In view of the fact that the two modes of fission have been observed experimentally with comparable probability in lighter fermium isotopes, in which valley I is expected to lie higher than in ^{264}Fm (see fig.4), one has to conclude that the probability of populating the valleys should be determined not at the scission point but at higher energies, somewhere near the fission barrier. One also has to make the reservation that the relative position in energy of the valleys is not well defined. In figs.3 and 4 the valleys are compared at the same value of $\alpha = 0.98$. Had we chosen another condition of comparison, the relative position of the valleys might have changed. But if the choice of the constraint is made from physical considerations like that associated with the thickness of the neck (see fig.5 and the corresponding discussion), this change hopefully should be small.

In ref./8/ only reflection symmetric shapes in the two-parameter-shape parameterization were considered and two symmetric valleys on the deformation energy surface have been found in nuclei near ^{264}Fm, which apparently correspond to our valleys I and III. The moments of the shape (r , σ) introduced in ref./8/ are, in ^{264}Fm, equal to (2.12, 0.76) and (2.86,1.20) for valleys I and III, respectively. The second point is located approximately in the "old" valley if we use the terminology of ref./8/ and the first lies near the "new" one, the centre-of-mass distance r being slightly larger (cf. fig.5b in ref./8/). While comparing one should keep in mind that the shape in valley I roughly corresponds to spheres separated by a distance of $\approx 0.27\, R_0$ between the tips rather than to two touching spheres.

In ref./9/ both reflection-symmetric and asymmetric shapes were considered in a simple parameterization of the nuclear shape with three parameters and the three valleys have also been found. The maximum semi-axes of nuclear shapes in valleys I , II and III for $\alpha = 0.98$ equal 14.3, 17.5 and 19.8 fm which roughly correspond to 14.4, 18.6 and 24 for the "super-short", "standard" and "super-long" channels respectively, in the terminology of ref./9/, but the details of the shapes are rather different (see also the discussion on this point in ref. /8/).

5. The properties of the fragment distributions in different valleys

If we divide the prescission nucleus conventionally into two fragments by a plane with a minimum area of the cross section , then in the case of the strongly shape-asymmetric mode II the fragments have the close numbers of nucleons, 130 and 134. These would be the most probable masses of the fragments if we assume that scission is most likely to take place in the narrowest part of the neck region.

Mode III is expected to have 138 and 120 nucleons in the fragments of ^{258}Fm under the same scission assumption. This is the only mode in which the number of nucleons in the heavy fragment is close to the value observed for the lighter nuclei. As a result, in all three modes the fission fragment mass distributions are practically symmetric.

The Coulomb interaction energy of the fragments, E_{int}^{Coul} , which was calculated as the total Coulomb energy of the whole nuclear body with subtraction of the Coulomb self-energy of each fragment separately is represented in fig.5 as a function of the parameter ϱ,

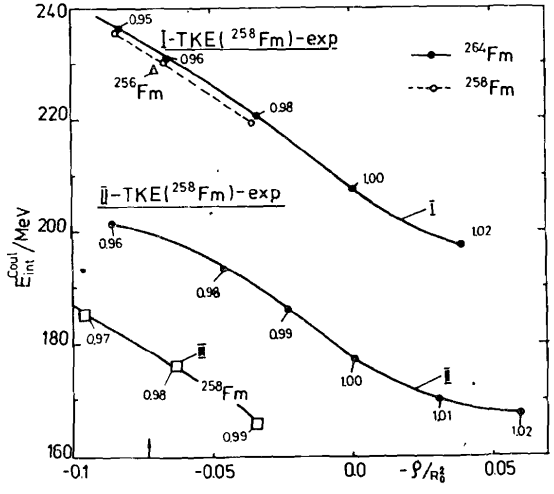

Fig.5
The fragment Coulomb interaction energy, E_{int}^{Coul} , as a function of the parameter ϱ defined in sect.3 for the three valleys I, II and III. The values of the parameter α are indicated by numbers near the points. The experimental data for TKE in the two modes of fission of ^{258}Fm are also given (exp) /1/.

which has been introduced in Sect.3. In fact, the quantity $-\varrho$ is plotted along the abscisa so that increasing $-\varrho$ in fig.5 corresponds to the evolution towards scission and postscission.
The choice of ϱ as a coordinate is motivated by the assumption that

scission of a nucleus in different valleys occurs at close values of the neck thickness. The value of the neck thickness that corresponds to the critical shape for which, according to the liquid-drop model, scission of the connected shape into two fragments takes place /23/, is marked by an arrow on the abscissa axis. The results of the calculations for ^{256}Fm and ^{258}Fm are also shown in the same figure together with experimental data for the observed total kinetic energy (TKE) (205 and 232 MeV) for the two modes of nuclear fission in ^{258}Fm /1/. The difference between the values of E_{int}^{Coul} calculated for valleys I and II is seen to be close to the TKE difference observed between the two fission modes and to be weakly dependent on the assumption of the scission point, i.e. almost constant in ϱ.

These are the two differences that are to be compared if one assumes the prescission kinetic energies to be the same in the two valleys. Moreover, if we assume that scission occurs at the critical value of the neck thickness /23/, then the values of E_{int}^{Coul} and TKE are close to each other in each valley. Under such an assumption very little is left for the prescission kinetic energy, which is supposed to be equal to the difference between TKE and E_{int}^{Coul}. The energy E_{int}^{Coul} of valley III is shown by squares in fig.5. A comparatively small TKE (176 MeV) is seen to correspond to this slightly asymmetric mode. This mode has not been observed so far. Experimentally one can discriminate between fission through the three different valleys by measuring the number of prompt neutrons presuming that a low excitation energy and, correspondingly, a small number of neutrons is associated with the spherical fragment but a high energy and a larger number of neutrons with the elongated one. This kind of measurement was carried out for the lighter nuclei of this region /24,25/.

6. Stability against variations in the number of nucleons in the fragments

In an attempt to understand the reason for the difference between the widths of the two mass distributions a calculation has been performed of the nuclear stability with respect to asymmetric shape variations in each of the three valleys. To this end, a constrained Hamiltonian was introduced instead of the formerly considered single-particle Hamiltonian H

$$H' = H - \lambda\eta , \qquad (7)$$

where λ is a Lagrange multiplier and $\eta=(A_H-A_L)/(A_H+A_L)$, $A_H(A_L)$ being the number of nucleons in the heavy (light) fragment, which is determined by the earlier described division of the prescission shape into fragments. For the Hamiltonian H' the same problem was solved as before for H and an example of the dependence on η of E is shown in fig.6. The difference $\Delta E = E - E_{min}$ for ^{264}Fm is seen to be close to a parabola with $\partial^2 E/\partial\eta^2$ equal to 2500–3000 MeV, the exact value being dependent on the points chosen to fit the parabola. Here E_{min} is a minimum value of E as a function of η. The E_{LD} is also shown. The liquid-drop stiffness $\partial^2 E_{LD}/\partial\eta^2$ corresponding to the minimum of the E value is seen not to contribute much to the total stiffness and the dependence of E_{LD} on η in the vicinity of the minimum of E is far from being quadratic, as predicted by the liquid-drop model for the region near the E_{LD} minimum with respect to η.

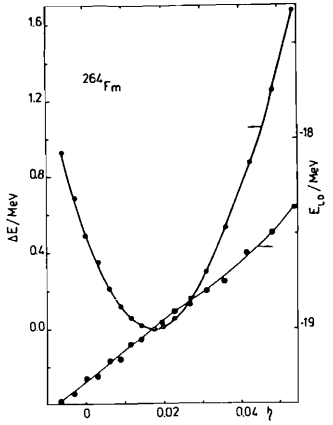

Fig.6.
The increment of the deformation energy $\Delta E = E - E_{min}$ (the left-hand scale) and the liquid-drop component of the energy, E_{LD} (the right-hand scale), as functions of the mass asymmetry parameter $\eta = (A_H - A_L)/(A_H + A_L)$. The minimum E_{min} is located in valley II. The parameter α =0.98.

For the quantity $\partial^2 E/\partial\eta^2$ in valley I, the obtained value lies within the same limits, while for valley III $\partial^2 E/\partial\eta^2$=2100 MeV.

The mass parameter $B_{\eta\eta}$ which corresponds to the degree of freedom η, calculated in the cranking model, equals 767 (1065) $\hbar^2$/MeV for valley I(II). With this mass parameter the zero-point oscillations of η near the equilibrium result in the fragment mass distribution with variance σ_η as

$$\sigma_\eta = \frac{1}{2}(A_H+A_L)\left[\hbar/\left(2\sqrt{B_{\eta\eta}\cdot\partial^2 E/\partial\eta^2}\right)\right]^{1/2} . \qquad (8)$$

By using the above-mentioned data we get theoretical estimates of FWHM for both valley I and II in the range (5–6) u, that is

in good agreement with the experimental value (7.5 u) for ^{258}Fm and ^{260}Md for the fission mode with the abnormally large TKE value and considerably smaller than the value corresponding to the other mode with the usual TKE value /1/. A small thermal excitation with temperature T=1 MeV that is close to the energy of the zero-point oscillations $\frac{1}{2}\hbar\omega_\eta = \frac{1}{2}\sqrt{(\partial^2 E/\partial\eta^2)/B_{\eta\eta}} = 0.9 - 1.0$ MeV results in the agreement between the theoretical and the experimental values of σ_η.

Thus, the quantum-mechanical uncertainty in the degree of freedom η is sufficiently large to understand the width of the mass distribution of the "fragment-shell-directed" mode of fission /1/. This new aspect, in addition to those already discussed in ref. /1/, of this unique mode of fission deserves special experimental and theoretical studies to be carried out. However, the difference between the mass distribution widths fails to be explained in the framework of the static approach used here. The theoretical difficulty in explaining the widths of the usual fragment mass distributions is also known to exist for other regions of nuclei.

7. Conclusions

The calculations of the deformation energy carried out using the Strutinsky method with the Woods-Saxon type potential and the multiparametric description of the nuclear shape indicate that in the vicinity of the scission point there exist three distinct valleys leading to almost symmetric fission. The valleys are well separated from each other by barriers and the Coulomb interaction energies of the fragments in two valleys near the assumed scission point are close to the measured TKE values for the two fission modes. The relative population of the valleys is determined at energies higher than those near the scission point. The width of the mass distribution of the "fragment-shell-directed" mode is mainly determined by the quantum-mechanical uncertainty of the coordinate in the corresponding degree of freedom and the distribution width of the usual mode remains unexplained in the static approach used here.

The most essential shortcoming of the theory seems to be the assumed constancy of the proton-to-neutron density ratio over the whole nuclear volume.

The author is grateful to V.G.Soloviev for continuous interest in the work and to Yu.Ts.Oganessian for stimulating discussions.

APPENDIX A

In the method used for calculating the single-particle spectrum /14-16/ the wave functions are expressed in terms of the eigenfunctions of a deformed harmonic oscillator. To achieve the required accuracy a comparatively large number of basis functions is needed in the region of the scission point, where the nuclear shape strongly deviates from an ellipsoid. To check the accuracy we compared in fig. 7(8) the protons (neutrons) single-particle spectra in the vicinity of the geometrical scission point (i.e. $\alpha = 1$) calculated with different numbers of the basis functions. It is seen that the usual

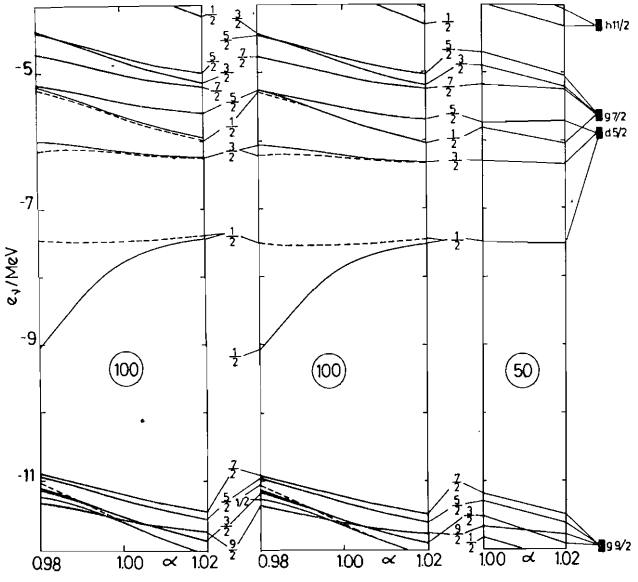

Fig.7. The proton single-particle levels along the bottom of valley I corresponding to the symmetric fission of almost spherical fragments. The nuclear shape at the point α = = 0.98 is shown in fig.2(I). The levels were calculated for the whole nucleus with usual (left) and high (centre) accuracy. The levels in a single separated fragment are given in the right section. The negative parity levels in the whole reflection-symmetric nucleus are given with dashed lines if they are distinguishable from the corresponding positive parity levels of the parity doublets, indicated by solid lines. If they coalesce, they are shown by one thick solid line. In the rightmost part of the figure the levels of the spherical fragment in the Coulomb field of the other fragment at a distance that corresponds to α = 1.02 are given. The splitting of the levels due to the Coulomb field are shown by the vertical size of the solid rectangle.

calculation with the number of eigenfunctions that roughly corresponds to about 16 shells in the spherical oscillator (the left section of the figs.) compares well with the spectrum calculated in an extended basis of about 23 shells (the central section).

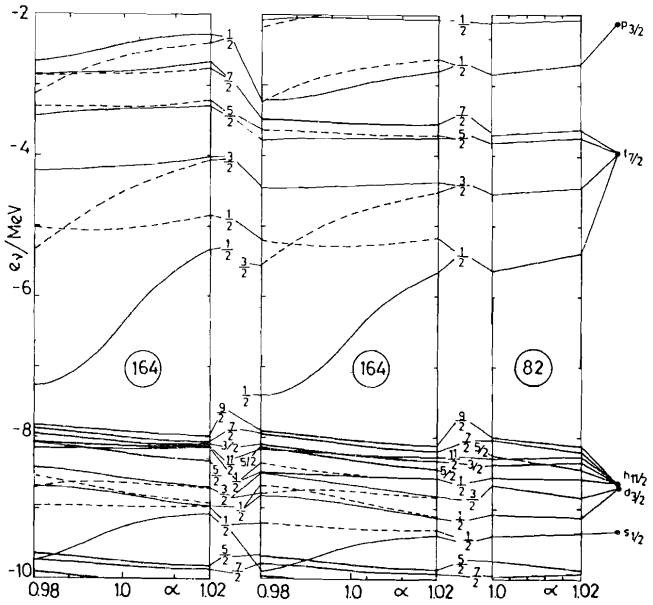

Fig.8

The same as in fig.7, but for neutrons. Because of the absence of the Coulomb field the levels in the rightmost part of the figure are degenerated exactly and shown by solid points.

Moreover, in this region there exists a possibility of checking the calculations by comparing the results with those obtained for a single fragment. After the scission ($\alpha > 1$) we decomposed the shape of a separate fragment in a series of Legendre polynomials as it was originally done for the whole nucleus (see eq. (4)), thereby treating one fragment as completely independent of the other, when calculating the neutron spectrum. For protons, we have, in addition, simulated the Coulomb potential of the other fragment by a point charge of an appropriate magnitude in the centre of mass of the other fragment. The results are shown in the right sections of figs. 7 and 8. Besides, in the rightmost parts of figs. 7 and 8, the spectra of spherical fragments are shown with the appropriate quantum numbers, the degeneracy of the proton spectrum being slightly removed by the Coulomb field of the other fragment.

By comparing this latter spectrum with the other spectra shown in figs. 7 and 8 one can see the impact of the deformation of the

fragment near the scission point on the spectra and classify the levels with the quantum numbers of approximately conserved angular momentum.

It is also seen that with separation of the fragments (i.e. with increasing α from 1 to 1.02) the positive- and negative-parity levels of the nucleus as a whole tend to be degenerated, the remaining splitting of the parity doublets being due to the nuclear interaction of the fragments. Indeed, the nuclear shape is understood here as an equipotential surface, on which the nuclear potential is equal to $V_0/2$, where V_0 is its value in the nuclear interior far from the nuclear surface. So, at the geometrical scission point in the neck region the nuclear potential is close to $V_0/2$, the fragments still interact with each other and the effect of this interaction on the single-particle spectrum is of some physical interest. This attractive interaction is concentrated near the centre of symmetry of the nucleus as a whole, i.e. in the neck region, and it therefore pushes down the energy levels of those states, which have a large probability for the nucleon to be found in the neck. These are the single-particle states with a large component of the wave function with a small value of the projection of the orbital angular momentum Λ on the nuclear symmetry axis and with an even oscillator quantum number n_z (the expression for the basis eigenfunctions is given in refs. [15,16]; in particular, the parity of a level is determined by the parity of the sum $n_z + \Lambda$). Accordingly, the maximum splitting of the parity doublets is seen in figs.7 and 8 for the levels with angular momentum projection $\Omega = 1/2$, the positive parity level being the lower one. An appreciable splitting is still seen for levels with $\Omega = 3/2$ with the lower member of the doublet being of negative parity. For doublets with large Ω the splitting rapidly dies down. Probably the most important result that follows from consideration of nuclear spectra in figs.7 and 8 is quantitative estimates of the number of neutrons in the neck region. It is seen that at the physical scission point ($\alpha \approx 0.98$, cf. fig.5 and the pertinent discussion) the neutron magic number is, contrary to expectations, equal to 166 rather than 164. This is confirmed by the calculation of the shell correction discussed below.

Once the shape of the fragment has become definite, it is possible to calculate its deformation energy (relative to the energy of the spherical fragment) which, for the elongation parameter α = = 1.00 (1.02) of the nucleus as a whole, equals 7.6 (5.0) MeV for an almost spherical fragment of valley I or II, and is 36(34) MeV for

an elongated fragment of valley II or III. Accordingly, for the whole nucleus with the same α value the deformation energy relative to the energy of infinitely far separated spherical fragments equals 15.2 (10) MeV in valley I, 43.6 (39) MeV in valley II, and 72(68) MeV in valley III.

We have also calculated the cranking-model mass parameters $B_{\bar{s}\bar{s}}$, where $\bar{s}$ symbolizes the distance between the fragments centres of mass, as it is changed during the descent along a fission valley (cf. the definition of $B_{\eta\eta}$ in sect.6). The results are shown in the table. One can see that in all three valleys the $B_{\bar{s}\bar{s}}$ values, as expected, are close to the asymptotic one for a completely separated fragment, that is almost equal to the reduced mass of the fragments.

APPENDIX B

To verify the validity of the Strutinsky method in the vicinity of the scission point the so-called "plateau condition" is to be checked [10,11,26,27]. In calculations with a finite-depth potential the bound-state levels are not sufficient to ensure a good plateau in the dependence of the shell-correction δE on the smearing width γ. The difficulty arises when the smooth part of the total nuclear binding energy is calculated as an average (defined specially) of the sums of the single-particle energies in one and the same single-particle potential up to the appropriate Fermi energies, rather than as an average of a set of binding energies of adjacent nuclei, calculated for each number of nucleons in the corresponding potential.

Such a substitution is an exact one (with an appropriate scale factor) for the Nilsson model and considerably facilitates calculations but one should complement the bound state levels by the properly chosen levels in the positive part of the spectrum. For the validity of the above-mentioned substitution these positive-energy levels should in a sense be an approximation to (an extrapolation of) the properly shifted and scaled bound state levels in heavier nuclei. Actually it is sufficient for the shell-correction method that the smoothed level density changes regularly in a transition from negative to positive energy levels [26,27].

From this point of view, good candidates for the positive-energy levels are the positive eigenvalues obtained by diagonalization of the Hamiltonian in a deformed harmonic-oscillator basis [26,27]. The parameters of the harmonic oscillator, in particular, the

oscillator frequency $\hbar\omega_0$, is usually chosen in such a way as to obtain the best approximation for the bound-state energies [15,16]. The desired accuracy may be achieved using $\hbar\omega_0$ from some interval. If we now impose the additional requirement of a regular behaviour of the smoothed level density in a transition from negative to positive energy levels, then, according to the calculation, we should choose the largest allowable value of $\hbar\omega_0$ [28]. It is especially important to follow this prescription in testing the convergence of δE with increasing dimension of the basis. If one fixes $\hbar\omega_0$ and increases the number of the basis functions, then the density of positive eigenvalues tends to infinity and, as a consequence, the plateau deteriorates [29]. But in choosing the maximum allowable value of $\hbar\omega_0$ for each number of the basis functions one can get a stable result, e.g. the one shown in fig.9,

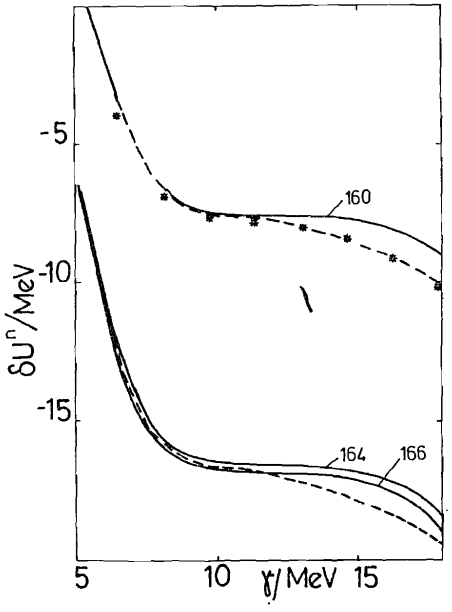

Fig.9.
The neutron shell correction δU^n as a function of the smearing width γ. The spectra in the extended (solid curves) and regular (dashed curves) basis were used (details of the spectra are given in the caption to fig.8). The doubled δU^n obtained with the spectrum of the single fragment is shown by stars for 80 neutrons. The numbers of neutrons in the nucleus as a whole are shown by the curves. The lower dashed curve corresponds to 164 neutrons. Pairing correction was not taken into account.

where the dependence of the neutron shell correction on the smearing width γ is shown for the regular calculation with approximately 16 oscillator shells (the dashed line; the corresponding single-particle spectrum is shown in fig.8, left section) and 23 shells (solid lines; the spectrum is given in fig.8, central section). The oscillator frequency $\hbar\omega_0$ was taken as $F/A^{1/3}$ with $F=53$ MeV in the former case and with $F = 80$ MeV in the latter. Also

shown is the doubled shell correction of the single fragment for 80 neutrons (stars). A very good and wide plateau is seen in the case of 23 shells, and the value of the shell correction in the regular case is close to that on the plateau at $\gamma \approx 1.0$ MeV. This value of γ was used in most of the calculations. It is also seen that the shell correction for 166 neutrons is smaller than for 164 neutrons, in accordance with the gap in the single-particle spectra described in Appendix A.

Table

Cranking model mass parameter $B_{\bar{3}\bar{3}}$ for the degree of freedom, associated with motion along a fission valley, in units of the reduced mass of the fragments. Labels I, II and III of the valleys are introduced in Sect.4

Valley \ α	0.98	1.00	1.01
I	1.35	1.14	1.05
II	1.93	1.53	1.08
III	1.14	1.22	1.02

References

1. Hulet E.K., Wild J.F., Dougan R.J., Lougheed R.W., Landrum J.H., Dougan A.D., Schädel M., Hahn R.L., Baisden P.A., Henderson C.M., Dupzyk R.J., Sümmerand K., Bethune G.R. Phys.Rev.Lett., 1986, 56, p.313.
2. Viola V.E., Kwiatkowski K. and Walker M. Phys.Rev. , 1985, C31, p.1550.
3. Itkis M.G., Okolovich V.N., Rusanov A.Ya., Smirenkin G.N. Z.Phys., 1985, A320, p.433.
4. Itkis M.G., Okolovich V.N., Rusanov A.Ya., Smirenkin G.N. Yad.Fiz., 1985, 41, p.849, 1109.
5. Pashkevich V.V. Nucl.Phys., 1971, A169, p.275.
6. Pashkevich V.V., Săndulescu A. JINR Rapid Communications No. 16-86, Dubna (1986) 19.

7. Pashkevich V.V. Proc. Int.School - Seminar on Heavy Ion Physics (Dubna, 1986), JINR, D7-87-68, Dubna, 1987, p.224.
8. Möller P., Nix J.R. and Swiatecki W.J. Proc.Int.School-Seminar of Heavy Ion Physics (Dubna, 1986), JINR, D7-87-68, Dubna, 1987, p.167; preprints LA-UR-86-3182 and LA-UR-86-3266.
9. Brosa U., Grossmann S., Müller A. Z.Phys., 1986, A325, p.241; Z.Naturforsch. , 1986, 41a, p.1341; Phillips-Universität preprint (1986).
10. Strutinsky V.M. Nucl.Phys., 1967, A95, p.420.
11. Strutinsky V.M. Nucl.Phys., 1968, A122, p.1.
12. Myers W.D., Swiatecki W.J. Ark.Fys., 1967, 36, p.343.
13. Myers W.D., Swiatecki W.J. Ann.of Phys., 1969, 55, p.395.
14. Pashkevich V.V., JINR, P4-4383, Dubna (1969).
15. Pashkevich V.V., Strutinsky V.M. Yad.Fiz., 1969, 9, p.56.
16. Damgaard J., Pauli H.C., Pashkevich V.V., Strutinsky V.M. Nucl.Phys., 1969, A135, p.432.
17. Ivanova S.P., Komov A.L., Malov L.A. and Soloviev V.G. Particles and Nuclei, 1976, 7, p.450.
18. Moon P., Spencer P.E. Field Theory Handbook (Springer, Heidelberg, 1961).
19. Hoffman D.C., Wilhelmy J.B., Weber J., Daniels W.R., Hulet E.K., Lougheed R.W., Landrum J.H., Wild J.F. and Dupzyk R.J. Phys.Rev., 1980, C21, p.972.
20. Mustafa M.G., Ferguson R.L. Phys.Rev., 1978, C18, p.301.
21. Wild J.F., Hulet E.K., Lougheed R.W., Baisden P.A., Landrum J.H., Dougan R.J. and Mustafa M.G. Phys.Rev., 1982, C26, p.1531.
22. Balagna J.P., Ford G.P., Hoffman D.C. and Knight J.D. Phys.Rev.Lett., 1971, 26, p.145.
23. Strutinsky V.M., Lyashchenko N.Y.; Popov N.A. Nucl. Phys., 1963, 46, p.639.
24. Balagna J.P., Farrell J.A., Ford G.P., Hemmendinger A., Hoffman D.C., Veeser L.R., Wilhelmy J.B. Proc.Third.Int.Atomic Energy Symposium on the Physics and Chemistry of Fission, Rochester, 1973 (IAEA, Vienna, 1974). Vol.2, p.191.
25. Hoffman D.C., Ford G.P., Balagna J.P. and Veeser L.R. Phys. Rev. , 1980, C21, p.637.
26. Brack M., Damgaard J., Jensen A.S., Pauli H.C., Strutinsky V.M., Wong C.Y. Rev.Mod.Phys., 1972, 44, p.320.
27. Brack M. and Pauli H.C. Nucl. Phys., 1973, A207, p.401.

28. Pashkevich V.V. Contributions to the 29th Conference on Nuclear Spectroscopy and Structure of Atomic Nuclei, Riga, 1979. (Leningrad, "Nauka", 1979), p.213.
29. Bolsterli M., Fiset E.O., Nix J.R. and Norton J.L. Phys.Rev., 1972, C5, p.1050.

Received by Publishing Department
on July 7, 1987.

Пашкевич В.В. E4-87-517

Предразрывные формы симметрично делящихся очень тяжелых ядер

Показано, что при теоретическом описании деления ядер в районе ^{264}Fm вблизи точки разрыва имеются три долины, ведущие к делению. Одна соответствует близко расположенным почти сферическим осколкам, другая - более удаленным друг от друга вытянутым осколкам. Имеется еще одна долина, в которой форма ядра близка к комбинации сферического и вытянутого осколка. Рассмотрены некоторые свойства массовых и энергетических распределений осколков.

Работа выполнена в Лаборатории теоретической физики ОИЯИ.

Препринт Объединенного института ядерных исследований. Дубна 1987

Pashkevich V.V. E4-87-517

Prescission Shapes of Symmetrically Fissioning Very Heavy Nuclei

It is shown that in the theoretical description of the fission process in the nucleus ^{264}Fm there turn out to be three valleys on the potential-energy surface in the region of the scission point. One valley corresponds to the compact configuration of two nearly spherical fragments; another, to more separated strongly elongated fragments. There still exists one more valley, in which nuclear shape is close to a combination of the spherical and elongated fragments. Some properties of the fragment mass and energy distributions are considered.

The investigation has been performed at the Laboratory of Theoretical Physics, JINR.

Preprint of the Joint Institute for Nuclear Research. Dubna 1987